Application of Effective Markovian Projection to SABR and Heston Models

Jacques Bagraim

A dissertation submitted to the Faculty of Commerce, University of Cape Town, in partial fulfilment of the requirements for the degree of Master of Philosophy.

May 23, 2023

MPhil in Mathematical Finance,
University of Cape Town.

Declaration

I declare that this dissertation is my own, unaided work. It is being submitted for the Degree of Master of Philosophy at the University of the Cape Town. It has not been submitted before for any degree or examination in any other University.

May 23, 2023

Abstract

Model flexibility is often at odds with tractable pricing, and models with tractable pricing often lack flexibility. This poses an issue when calibrating a model to market data where tractability and flexibility are both required. We investigate an approach that allows one model to be projected onto another, potentially allowing for a flexible model to be represented by a tractable one. Here, Effective Markovian Projection is used to obtain equivalent Heston model parameters from a range of SABR models with different skew parameters using two distinct point-matching algorithms. The implied parameters are used to price European claims under a variety of schemes in order to outline the efficacy in this context. We see that this technique is accurate when the underlying probability densities of both models match closely, i.e., when the SABR skew parameter approaches unity, as is seen by comparing prices of claims using Classic Markovian Projection where the underlying SABR processes share the same density. PDE and perturbation SABR prices match closely while Heston characteristic function prices become unstable at lower skew parameters and far in-the-money and out-the-money values of the strike. Lastly, a potential improvement to this application involving error-correction terms is proposed for further application.

Acknowledgements

I would like to firstly thank my supervisor, Professor Thomas McWalter for his interest in and dedication to my success in this endeavour. I would like to acknowledge all the AIFMRM teaching and administrative staff for their tireless efforts in the teaching and dissertation process, as well as my class mates for their collective support of me and one another throughout this demanding year. I would like to thank and acknowledge my partner, Erin, for her endless support and commitment to me and for her consistent love and affection when it was needed the most.

Contents

List of Figures

List of Tables

Chapter 1

Introduction

In the field of Mathematical Finance *many* stochastic models exist. Each aims to capture observed market phenomena more accurately and realistically than the next, and each have their own advantages and disadvantages and thus play individual roles in different areas of derivatives pricing and hedging as well as risk management. In the field of volatility modelling, early work on local volatility was pioneered by Dupire (1994) and Derman and Kani (1994) which aimed to account for the so-called market 'smile' of implied option volatility with varying strike price. This local volatility model did not, however, shed light on the dynamics of the underlying volatility through time. Early work on stochastic volatility/variance modelling was pioneered by Heston (1993), followed by more recent work on stochastic volatility models, namely the Stochastic Alpha Beta Rho (SABR) model and its variants developed by Hagan *et al.* (2002). Often in practice a chosen model is used because of its simplicity in that its parameters are easily estimated/measured from market data and its governing mathematics fairly straightforward, but would fall short in its ability to accurately price contingent claims with computational efficiency or would have the disadvantage of being poorly tractable. On the other hand, another model could have inherent pricing efficiencies but fall short in that its parameters are difficult to measure and calibrate from market data. The goal then of market practitioners and researchers alike, is to develop methods to make use of the advantages of two (or more) models while avoiding their inherent disadvantages.

The seminal work by Gyöngy (1986) allows a one dimensional Itô process to be estimated from a multi-dimensional Itô process, where these two processes share the same marginal terminal probability distribution. The idea here is that this new process is driven by a *single* Brownian motion and has a marginal probability density the same as the multi-dimensional process. In essence, a multi-dimensional Itô

process is 'mapped' onto a single-dimensional framework. The way this is applied is by rewriting the original process in a local volatility form by combining appropriate terms and computing one or more conditional expectations to obtain the new process parameters. This can be performed in a variety of ways — Piterbarg (2006) introduce the idea of Gaussian approximations wherein the dynamics of the process needing to be projected are approximated as a Gaussian process. This allows for a great simplification of the conditional expectations needing to be solved and is a reasonable approximation as long as the local volatility function of this process is linear or close to linear in terms of the underlying asset — this is the case in all the applications explored here. Along with Gaussian process approximations, parameter averaging techniques introduced by Piterbarg (2005) are used to evaluate the projected model parameters. The combination of these two techniques is known as 'Markovian Projection' (MP) or 'Classic Markovian Projection' and is applied to valuing financial products of varying complexity, from options on indices in a local volatility model to options on multiple underlying rates with stochastic volatility. The theory behind this and a worked example is summarised in Section 4.

Felpel *et al.* (2022) develop a novel methodology to perform this model projection. They aim to project two or more models onto their own one-dimensional framework and to solve for an undefined model's parameters in terms of a known model's parameters by equating their local volatility functions. To solve the conditional expectations outlined by Gyöngy's lemma, expressions for the terminal densities of the underlying assets in the models in question are determined by developing and solving effective forward (Kolmogorov) equations (Hagan (2015), Felpel *et al.* (2021)). Next, point matching algorithms are developed to imply the new model parameters from the known model's parameters. This combination of techniques is coined 'Effective Markovian Projection' (EMP) and is used to project displaced SABR (dSABR), normal SABR (nSABR) and ZABR models for pricing of options on mid-curves and constant maturity swap (CMS) spreads. The theory behind this is discussed briefly in Section 2.

For our purpose, we consider general time-homogenous stochastic volatility models of the form

$$\begin{cases} dF_t = V(v_t)C(F_t)dW_t^{(1)}, & F_{t_0} = f \\ dv_t = \mu(v_t)dt + \nu(v_t)dW_t^{(2)}, & v_{t_0} = \alpha \\ d\langle W^{(1)}, W^{(2)}\rangle_t = \rho dt, \end{cases} \tag{1.1}$$

where $V(\cdot)$ is a function of the volatility process, $C(\cdot)$ is the *back-bone* function of the forward, such as a function of a forward rate or forward stock price, $\mu(\cdot), \nu(\cdot)$

are functions specifying the volatility/variance dynamics, and $W_t^{(1)}, W_t^{(2)}$ are two correlated Brownian motions with correlation ρ. This general form covers all the models that this work will refer to and most stochastic volatility models in general. Specifically, this dissertation applies EMP to map a calibrated SABR model with defined parameters, and an undefined Heston model onto a single-dimensional framework using the result from Gyöngy (1986). This is done to obtain the unknown Heston model parameters from a range of SABR model parameters by equating expressions for their respective mapped densities. Using these implied parameters as well as the original model parameters, European call option prices are evaluated using a variety of pricing techniques. The efficacy of the EMP technique, effect of the model parameters on the various pricing schemes, and general applicability of this technique to the Heston and SABR models are all explored and discussed. Chapter 2 deals with the general mathematical theory of Stochastic Integration and distribution mimicking and discusses the two matching algorithms used to imply the Heston parameters as well as the mathematical theory behind option pricing under various pricing schemes, namely perturbation expansions, characteristic functions and partial differential equation (PDE) pricing. Chapter 3 explores the theory behind classic Markovian Projection and applies this technique to valuing an option on a CMS spread in order to compare the MP and EMP techniques. Chapter 4 deals with the numerical results, specifically the direct results of Effective Markovian Projection — the implied Heston model parameters, as well as a comparison of the matching techniques used to obtain them. This chapter also deals with a comparison of European call option prices under both models using the various pricing schemes and the efficacy of EMP under different values of the SABR skew parameter. Chapter 5 draws on all the main aspects of this dissertation and concludes the results.

Chapter 2

General Mathematical Background

In this chapter the basic mathematics and algorithmic approaches behind the EMP technique are outlined. First, distribution mimicking and model projection are discussed. Transition densities are then introduced in order to evaluate the projected variance (a conditional expectation) of both models under analysis. Lastly, point matching algorithms — algorithms to match the projected variances of both models — are discussed.

2.1 *Stochastic Analysis*

For the entirety of this work we shall consider and be working with the stochastic basis $(\Omega, \mathcal{F}, \{\mathcal{F}_t\}_t, \mathbb{P})$ satisfying the usual conditions, where $\mathbb{P}$ is the real-world measure and $t \in [0, T]$[1]. We consider our sample space, Ω to be an n-dimensional real space $\mathbb{R}^n$. Lastly, the probability space is equipped with a d-dimensional Brownian Motion, W_t, which generates the natural augmented filtration $\mathcal{F}_t$ i.e., such that

$$\mathcal{F}_t = \sigma\{W_u | u \leq t\}.$$

On this basis we consider general Itō processes, X_t, of the form

$$dX_t = \mu(t, X_t)dt + \sigma(t, X_t)dW_t, \tag{2.1}$$

with adapted coefficient functions $\mu : [0, T] \times \mathbb{R}^n \to \mathbb{R}^n$ and $\sigma : [0, T] \times \mathbb{R}^n \to \mathbb{R}^{n \times d}$. Here, these coefficient functions satisfy

$$\int_0^T |\mu(s, x)| ds < \infty, \qquad \int_0^T |\sigma(s, x)|^2 ds < \infty \ \ a.s.$$

[1] Here, T is the finite maturity of the claim (fitting maturity) under evaluation in each model.

2.1.1 *Distribution Mimicking*

Here the seminal work of Gyöngy (1986) is introduced.

Theorem 2.1. *For an Itō process X_t on the probability space $(\Omega, \mathcal{F}, \mathbb{P})$ admitting a **unique** solution and having the following dynamics*

$$dX_t = \alpha(t,\omega)dt + \beta(t,\omega)dW_t, \tag{2.2}$$

where α, β are bounded, adapted processes and $\beta\beta^T$ is uniformly positive definite, there exists another process x_t having the following dynamics

$$dx_t = a(t,x_t)dt + b(t,x_t)d\tilde{W}_t, \tag{2.3}$$

with non-random coefficients where

$$a(t,x_t) = \mathbb{E}[\alpha(t,\omega)|X_t = x_t], \tag{2.4}$$

$$b(t,x_t)^2 = \mathbb{E}[\beta(t,\omega)\beta(t,\omega)^T|X_t = x_t], \tag{2.5}$$

such that x_t has the same one-dimensional marginal distribution as X_t for all $t \in [0,T]$.

Remark 1. Many stochastic volatility models, including the SABR and Heston-type models considered here, do not have unique solutions to their corresponding Itō diffusive SDEs — see (Oskendal, 2000, p. 66) for conditions under which uniqueness may be guaranteed. It should be noted that the result above requires that the solutions to the SDE with stochastic coefficients be **unique** in order for the theorem to hold. More recent work done by Kumar (2013) outlines a methodology to determine, under certain conditions, unique strong solutions to degenerate SDEs with non-Lipschitz coefficients. This allows the application of Markovian Projection to the SDE types mentioned above.

2.2 *Projected Variance*

Consider two models, one which is calibrated to market data and who's model coefficients have been determined, and the other who's coefficients we'd like to determine. If one is able to project these models onto a deterministic framework by using Theorem 2.1 and determine expressions for the coefficients a and b, one can infer the values of the second model's coefficients from the first, without having to calibrate this model directly. This means that one can calibrate one model and price in another with consistency and accuracy – the best of both worlds. The purpose then, is to evaluate the conditional expectations in (2.4) and (2.5).

In order to determine the projection model parameters from the base model parameters, both models are projected onto a deterministic framework as outlined by Theorem 2.1 in order to determine expressions for $b(t, x_t)^2$, referred to as the projected variance, σ^2_{proj}. This is done by evaluating the conditional expectation in (2.5) for both models.

Consider a time t where $v_t = A$ and $F_t = F$, then

$$\begin{aligned}\sigma^2_{\text{proj}} &= C(F)^2 \frac{\mathbb{E}[V(A)^2 \mathbb{I}_{\{F_t = F\}}]}{\mathbb{E}[\mathbb{I}_{\{F_t = F\}}]} \\ &= C(F)^2 \frac{\int_0^\infty V(A)^2 p(t_0, f, \alpha, t, F, A) dA}{\int_0^\infty p(t_0, f, \alpha, t, F, A) dA} \\ &= C(F)^2 \frac{Q^{(2)}(t_0, f, \alpha, t, F)}{Q^{(0)}(t_0, f, \alpha, t, F)}.\end{aligned} \tag{2.6}$$

Here, $C(\cdot)$ and $V(\cdot)$ are defined in (1.1), and the function $Q^{(k)}$ is the volatility/variance moment and is defined by

$$Q^{(k)} := \int_0^\infty V(A)^k p(t_0, f, \alpha, t, F) dA, \tag{2.7}$$

and

$$p(t, F) = Q^{(0)}(t_0, f, \alpha, t, F)$$

where $p(t_0, f, \alpha, t, F, A)$, or equivalently $p(t, F)$, is the *effective* transition probability density of the underlying forward of moving from state (f, α) at time t_0 to (F, A) at time t. This is defined as

$$p(t, F) dF = \mathbb{P}[F < \tilde{F}_t < F + dF | \tilde{F}_{t_0} = f, \nu_{t_0} = \alpha]. \tag{2.8}$$

Hagan *et al.* (2002) analyse the system of equations in (1.1) in the context of the SABR model using singular perturbation techniques derived from perturbation theory. Using a perturbation parameter, ϵ, the equations in (1.1) can be written as

$$\begin{cases} d\tilde{F}_t = \epsilon V(v_t) C(\tilde{F}_t) dW_t^{(1)}, & \tilde{F}_{t_0} = f \\ dv_t = \mu(v_t)dt + \epsilon\nu(v_t)dW_t^{(2)}, & v_{t_0} = \alpha \\ d\langle W^{(1)}, W^{(2)}\rangle_t = \rho dt. \end{cases} \tag{2.9}$$

The idea here is that a forward Kolmogorov equation which relies on the parameters in (2.9) as well as ϵ can be derived but whose solution at a limiting value of ϵ differs from the limit of the general solution to the said PDE – namely, the limit is singular. The density of the forward, F, satisfies the forward Kolmogorov equation

$$\partial_t p(t,F) = \partial_{FF}[D(t,F)p(t,F)] \tag{2.10}$$

$$p(t_0, f) = \delta(F - f),$$

where $D(\cdot,\cdot)$ is a function depending on the model parameters and time. Felpel *et al.* (2021) show that using the parameter ϵ as well as the the volatility moments defined in (2.7), (2.10) can be written as

$$\partial_t Q^{(0)}(t,F) = \frac{1}{2}\epsilon^2 \partial_{FF}[C(F)^2 Q^{(2)}(t,F)], \tag{2.11}$$

$$Q^{(0)}(t,F) \to \delta(F-f) \quad \text{as } t \to t_0^+.$$

Using the density p of forward F, we can define the prices of European calls and puts as

$$\text{Call}_p(T,F) = \int_K^\infty (F-K)p(T,F)dF, \tag{2.12}$$

and

$$\text{Put}_p(T,F) = \int_{-\infty}^K (K-F)p(T,F)dF. \tag{2.13}$$

Hagan (2015) develops a finite difference scheme using (2.12) and (2.13) to specify the boundary grid behaviour to numerically solve (2.11). After this is done, ϵ is set back to 1 and the result retained. Felpel *et al.* (2021) give a general representation of (2.11) by solving for the $Q^{(2)}$, which reduces to

$$\partial_t p(t,F) = \frac{1}{2}a(t)^2\partial_{FF}\left[C(F)^2 p(t,F)e^{G(t)}(1+2b(t)z(F)+c(t)z(F)^2)\right], \tag{2.14}$$

$$p(t,F) \to \delta(F-f) \quad \text{as } t \to t_0^+,$$

where the coefficients a, b, c, z and G are process-specific. Getting back to (2.6), we have the following proposition.

Proposition 2.2. *Given a general stochastic volatility model of the form in* (1.1) *satisfying certain assumptions outlined in Felpel et al. (2021) and given explicitly in Appendix A, the projected variance is approximated as*

$$\sigma^2_{\text{proj}}(t,F) \approx C(F)^2 a(t)^2 e^{G(t)}(1+2b(t)z(F)+c(t)z(F)^2), \tag{2.15}$$

where a, b, c, z and G are specified in Appendix A for both the SABR and Heston models.

2.3 *Matching Techniques*

To illustrate the proceeding working, consider a SABR process of the form

$$\begin{cases} dF_t = (F_t)^\beta v_t dW_t^{(1)}, & F_{t_0} = f \\ dv_t = \nu v_t dW_t^{(2)}, & v_{t_0} = \alpha \\ d\langle W^{(1)}, W^{(2)}\rangle_t = \rho dt, \end{cases} \tag{2.16}$$

and a Heston process of the form

$$\begin{cases} d\tilde{F}_t = \sqrt{\tilde{v}_t}\tilde{F}_t d\tilde{W}_t^{(1)}, & \tilde{F}_{t_0} = \tilde{f} \\ d\tilde{v}_t = \kappa(\Lambda - \tilde{v}_t)dt + \tilde{\nu}\sqrt{\tilde{v}_t}dW_t^{(2)}, & \tilde{v}_{t_0} = \tilde{\alpha} \\ d\langle \tilde{W}^{(1)}, \tilde{W}^{(2)}\rangle_t = \tilde{\rho}dt. \end{cases} \tag{2.17}$$

For the SABR process, β is the skew parameter and influences the distribution of the underlying forward F as well as the implied volatility smile produced, ν is the volatility of the volatility, or *volvol* and plays a similar role to the constant volatility σ in the Black-Scholes framework, although acting on the volatility dynamics and not the dynamics of a single stock. In Heston's original formulation there is assumed to be a zero correlation between the forward and the variance — we use a flat correlation to more realistically represent the observed market data in terms of implied volatility smiles. The long-run average (mean) of the variance is represented by Λ while κ is the mean-reversion rate. Here, the Heston model's parameters are marked with a tilde since it is the projection model. As is convention when

dealing with stochastic volatility models, one considers only the forward value, F_t and ignores the drift component of the diffusion. One can reintroduce discounting with an arbitrary term structure, if necessary. For the SABR process as per (1.1), $C(F) = (F_t)^\beta$ and for the Heston process, $\tilde{C}(F) = \tilde{F}_t$. We have a fully specified SABR process and can thus determine a closed form expression for it's projected variance, $\sigma^2_{\text{proj}}(t, F)$ as in (2.15). We would then like to evaluate an expression for the projected variance of the Heston process (the projection model) in terms of the SABR process. To do this we need to specify an appropriate fitting maturity T. Once this is done, we can imply the projection model parameters and use these for pricing. In this case, we are implying the Heston model parameters $\tilde{\rho}, \tilde{\alpha}, \tilde{\nu}$ from the known SABR parameters ρ, α, ν. After these are determined, we use an optimization routine in order to solve for the remaining Heston parameter $\tilde{\kappa}$. As is similarly outlined in Felpel *et al.* (2022), we work with the expression

$$\tilde{\sigma}_{\text{proj}}(t, F)^2 = \tilde{C}(F)^2 \hat{a}(t)(1 + 2\tilde{b}(t)\tilde{z}(t) + \tilde{c}(t)\tilde{z}(F)^2), \tag{2.18}$$

where $\hat{a}(t)$ is defined as

$$\hat{a}(t) := \frac{C(f)^2}{\tilde{C}(f)^2} a(t)^2 e^{G(t)}. \tag{2.19}$$

This expression greatly simplifies the computation of the parameter $\tilde{\alpha}$ as will be shown.

2.3.1 *At-the-money matching*

Since the coefficient functions $\tilde{C}(\cdot)$ and $\tilde{z}(\cdot)$ are specified prior to projection, we need to match the coefficients $\hat{a}(\cdot), \tilde{b}(\cdot)$ and $\tilde{c}(\cdot)$. We can see that we will need at least three equations to do this. Here we assert that the at-the-money (ATM) values of the projected variances of both models are equal, as well as their first and second derivatives. Thus we have

$$\begin{aligned} &\sigma^2_{\text{proj}}(t, f) = \tilde{\sigma}^2_{\text{proj}}(t, f) \\ &\partial_F \sigma^2_{\text{proj}}(t, f) = \partial_F \tilde{\sigma}^2_{\text{proj}}(t, f) \\ &\partial_{FF} \sigma^2_{\text{proj}}(t, f) = \partial_{FF} \tilde{\sigma}^2_{\text{proj}}(t, f). \end{aligned} \tag{2.20}$$

Once these expressions are properly evaluated the projection model coefficient functions are given in Felpel *et al.* (2022) as

$$\tilde{b}(t) = \frac{\tilde{C}(f)}{C(f)}\big(C_F(f) + b(t)\big) - \tilde{C}_F(f) \tag{2.21}$$

$$\begin{aligned} \tilde{c}(t) = \frac{\tilde{C}(f)^2}{C(f)^2}\big(C_F(f)^2 + C_{FF}(f)C(f) + 3C_F(f)b(t) + c(t)\big) \\ - \tilde{C}_F(f)^2 - \tilde{C}_{FF}(f)\tilde{C}(f) - 3\tilde{C}_F(f)\tilde{b}(t). \end{aligned} \tag{2.22}$$

2.3.2 *Minimal point matching*

Here we specify two additional points, F_1 and F_2, at which the projected variances of both models agree. These two points are *typically* in-the-money ITM and out-the-money OTM points of the forward. As will be seen, the specification of these additional two points allows better fitting of the projected variances at the far ITM and OTM values. As before $\hat{a}(t)$ is given by (2.19). The additional two coefficients are given by Felpel *et al.* (2022) as

$$\tilde{b}(t) = \frac{1}{2}\frac{r(t,F_1)\tilde{z}(F_2)^2 - r(t,F_2)\tilde{z}(F_1)^2}{\tilde{z}(F_1)\tilde{z}(F_2)^2 - \tilde{z}(F_1)^2\tilde{z}(F_2)} \tag{2.23}$$

$$\tilde{c}(t) = \frac{r(t,F_2)\tilde{z}(F_1)^2 - r(t,F_1)\tilde{z}(F_2)}{\tilde{z}(F_1)\tilde{z}(F_2)^2 - \tilde{z}(F_1)^2\tilde{z}(F_2)}, \tag{2.24}$$

where

$$r(t,F) = \frac{C(F)^2\tilde{C}(f)^2}{\tilde{C}(F)^2C(f)^2}(1 + 2b(t)z(F) + c(t)z(F)^2) - 1. \tag{2.25}$$

2.4 *Contingent Claims Pricing*

In this section we discuss various pricing techniques for claims where the underlying forward follows a SABR or Heston-type process. The perturbation expansion formula for the implied forward volatility is widely used by market practitioners because of its accuracy over realistic strike ranges as well as its computational ease of implementation. The arbitrage-free SABR pricing technique is used as a comparison to the perturbation expansion pricing but is computationally expensive and complex to implement although it is used when analytical pricing formulae do not exist. The Heston characteristic function pricing technique is widely used for its speed and accuracy, assuming the model parameters are as they should be. It is well documented that this technique is sensitive to option parameters as well as model parameters and can often lead to inaccurate or unrealistic prices if these are not correctly specified. Lastly, Monte-Carlo prices are used for comparison to the characteristic function prices and to outline the above-mentioned sensitivities.

2.4.1 *Perturbation expansion*

Hagan *et al.* (2002) obtain an expression for the Black-implied volatility, σ_{impl}, of an underlying forward in terms of the strike price, K, using perturbation/asymptotic expansion of the parameter ϵ in the original model. First, the expression for the

implied volatility when $0 < \beta < 1$ is as follows

$$\sigma_{\text{impl}}(K) = \frac{\epsilon\alpha}{(fK)^{\frac{1-\beta}{2}}} \frac{1}{\left[1 + \frac{(1-\beta)^2}{24}\log\left(\frac{f}{K}\right)^2 + \frac{(1-\beta)^4}{1920}\log\left(\frac{f}{K}\right)^4 + ...\right]} \left(\frac{\zeta}{\hat{\chi}(\zeta)}\right) \cdot\left\{1 + \left[\frac{(1-\beta)^2\alpha^2}{24(fK)^{1-\beta}} + \frac{\rho\alpha\nu\beta}{4(fK)^{\frac{1-\beta}{2}}} + \frac{2-3\rho^2}{24}\nu^2\right]\epsilon^2 T + \cdots\right\}.$$

For the log-normal case when $\beta = 1$,

$$\sigma_{\text{impl}}(K) = \epsilon\alpha\frac{f-K}{\log\left(\frac{f}{K}\right)}\left(\frac{\zeta}{\hat{\chi}(\zeta)}\right)\left\{1 + \left[-\frac{\alpha^2}{24} + \frac{\rho\alpha\nu}{4} + \frac{(2-3\rho^2)\nu^2}{24}\right]\epsilon^2 T + \cdots\right\},$$

where

$$\zeta = \frac{\nu}{\alpha}\sqrt{(fK)}\log\frac{f}{K} \qquad \hat{\chi}(\zeta) = \log\left(\frac{\sqrt{1-2\rho\zeta+\zeta^2} - \rho + \zeta}{1-\rho}\right).$$

The prices of claims are then computed in terms of the strike using Black's formula in conjunction with the above implied volatilities as follows,

$$c(K) = f\Phi(d_1(K)) - K\Phi(d_2(K)),$$

where

$$d_{1,2}(K) = \frac{\log\left(\frac{f}{K}\right) \pm \frac{1}{2}\sigma_{\text{impl}}(K)^2 T}{\sigma_{\text{impl}}(K)\sqrt{T}}$$

and $\Phi(\cdot)$ is the distribution function of a normal random variable.

2.4.2 *Arbitrage-free SABR*

The analytical expression for the implied volatility mentioned above is not arbitrage-free since in the original SABR model the forward probability density can be negative for low strikes and long dated maturities. Le Floc'h and Kennedy (2014) implement a finite difference technique (Lawson and Swayne (1976)) for solving the density, Q, in the Fokker-Planck/Kolmogorov forward PDE outlined by Hagan *et al.* (2014). This density is then used to price claims.

$$\frac{\partial Q}{\partial t}(t,F) = \frac{\partial^2 M(t,F)Q(t,F)}{\partial F^2},$$

with initial condition

$$\lim_{t\to 0} Q(t,F) = \delta(F-f),$$

where δ is the Dirac-delta function and

$$M(t,F) = \frac{1}{2}D^2(F)E(t,F), \qquad E(t,F) = e^{\rho\nu\alpha\Gamma(F)t}, \qquad \Gamma(F) = \frac{F^\beta - f^\beta}{F-f}$$
$$D(F) = \sqrt{\alpha^2 + 2\alpha\rho\nu y(F) + \nu^2 y(F)^2}F^\beta, \qquad y(f) = \frac{F^{1-\beta} - f^{1-\beta}}{1-\beta}.$$

Once this density is solved for, prices of claims are computed using the Breeden-Litzenberger formula (Breeden and Litzenberger (1978)).

$$V_{\text{call}}(t,K) = \int_K^{F_{\max}} (F-K)Q(t,F)dF + (F_{\max}-K)Q_R(T),$$

where $Q_R(T)$ is the accumulated density at the upper boundary, i.e., when $F = F_{\max}$, and is given by

$$\frac{\partial Q_R}{\partial T}(t) = \lim_{F\to F_{\max}} \frac{\partial M(t,F)Q(t,F)}{\partial F}.$$

Clearly we restrict ourselves to positive forward values since our forward is a single stock. Recently there has been more interest and work done on negative interest rates due to their increasing pervasiveness in many markets. Le Floc'h and Kennedy (2014) outline techniques to solve a 'Free-Boundary SABR' PDE which allows for this, although this is not discussed here.

2.4.3 *Heston characteristic function*

The price of a call option for a forward F with a time t_0 value of f, may be written as

$$V_{\text{call}}(K) = f\mathbb{E}^{\mathbb{Q}_{\tilde{F}}}[\mathbb{I}_{F_T>K}] - K\mathbb{E}^{\mathbb{Q}}[\mathbb{I}_{F_T>K}].$$

Here, $\tilde{F} = \log(F)$, $\mathbb{Q}$ is the risk-neutral measure and the measure $\mathbb{Q}_{\tilde{F}}$ is defined as

$$\frac{d\mathbb{Q}_{\tilde{F}}}{d\mathbb{Q}} = \frac{F_T}{f},$$

by a change of numéraire and since the risk-neutral rate, r, is zero. These expectations may be thought of as probabilities and may be written as

$$\begin{aligned} V_{\text{call}}(K) &= f\mathbb{Q}_s\{F_T > K\} - K\mathbb{Q}\{F_T > K\} \\ &= fP_1 - KP_2. \end{aligned}$$

By McWalter (2021), the probabilities P_1 and P_2 are given by

$$P_1 = \frac{1}{2} + \frac{1}{\pi}\int_0^\infty \text{Re}\left[\frac{e^{-iuk}\phi_{\tilde{F}_T}(u-i)}{iu\phi_{\tilde{F}_T}(-i)}\right]du,$$
$$P_2 = \frac{1}{2} + \frac{1}{\pi}\int_0^\infty \text{Re}\left[\frac{e^{-iuk}\phi_{\tilde{F}_T}(u)}{iu(-i)}\right]du,$$

where $k = \log(K)$ and $\phi_X(u)$ is the characteristic function of a random variable X. This result uses the inversion theorem proven by Gil-Pelaez (1951) for a general random variable X with characteristic function ϕ_X. Here, we consider log-normally distributed random variables with characteristic function given as

$$\phi_X(u) = \exp\left(iu\left(\log(X_0) + \left(r - \frac{1}{2} v_{t_0}^2 \right) T \right) - \frac{1}{2} v_{t_0}^2 T u^2 \right),$$

Where, $v_{t_0} = \tilde{\alpha}$. For pricing claims under the Heston model we use a characteristic function defined by Albrecher *et al.* (2007) which is numerically more stable over a wider strike and maturity range than the expression given here.

Chapter 3

Classic Markovian Projection — a Warm-Up

3.1 *Approximating Multi-Dimensional SABR Processes*

Often in practice a claim depends on more than one underlying asset. Each of these assets is driven by its own diffusion and parameters. Pricing using multi-dimensional PDEs is often computationally cumbersome and difficult to implement. So, we need a way to 'singularise' the dimension of the problem in order to apply classic pricing techniques, without losing any of the characteristics of the original diffusion.

Here we outline the theory behind the approximation of a two-dimensional SABR diffusion as is found in detail for $n \in \mathbb{N}$ assets in Kienitz and Wittke (2010). A two-asset SABR process for each forward $F_{i,t}$ with $i, j \in \{1, 2\}$ is given as

$$\begin{cases} dF_{i,t} = v_{i,t} C_i(F_{i,t}) dW_{i,t}^{(1)}, & F_{i,t_0} = f_i, \\ dv_{i,t} = \nu_i v_{i,t} dW_{i,t}^{(2)}, & v_{i,t_0} = \alpha_i, \\ \text{where,} \\ d\langle W_i^{(1)}, W_j^{(2)} \rangle_t = \gamma_{ij} dt, \\ d\langle W_1^{(1)}, W_2^{(1)} \rangle_t = \rho dt, \\ d\langle W_1^{(2)}, W_2^{(2)} \rangle_t = \xi dt. \end{cases} \tag{3.1}$$

Here, as before, $C_i(\cdot)$ is a suitably chosen 'back-bone' function and in the case of the general SABR model (used here) is given as $F_{i,t}^{\beta_i}$, ρ is the correlation between the two forwards, γ_{ij} are the cross-correlations between the forwards and volatilities and ξ is the correlation between the two forward volatilities.

We now consider the difference between two assets and choose a SABR-style model of the form,

$$\begin{cases} dF_t = u_t C(F_t) dB_t^{(1)}, & F_{t_0} = f = f_1 - f_2 \\ du_t = \nu u_t dB_t^{(2)}, & u_{t_0} = 1 \\ \text{where,} \\ d\langle B^{(1)}, B^{(2)} \rangle_t = \gamma dt. \end{cases} \tag{3.2}$$

Here, γ is the correlation between the 'combined' forward (spread) and its volatility process and $u_{i,t} = \frac{v_{i,t}}{\alpha_i}$. We impose that the new back-bone function is given as a displaced diffusion of the form

$$C(F_t) = p + q(F_t - f), \tag{3.3}$$

where

$$p = C(f), \tag{3.4}$$

$$q = C'(f), \tag{3.5}$$

for reasons which will become apparent in the next section. Since the process for F_t itself is not an Itô diffusion because of its reliance on feedback from u_t, we would like to map it onto a diffusion in order to apply the result from Gyöngy (1986). To begin, we consider a local volatility model of the form

$$dF_t = \sigma(t) dB_t^{(1)}, \tag{3.6}$$

in order to be able to apply Theorem 2.1. By imposing the form of (3.2) we approximate the variance of the spread, $\sigma^2(t)$ as

$$\sigma^2(t) = \mathbb{E}[(F_{1,t} - F_{2,t})^2] \tag{3.7}$$

$$\approx u_{1,t}^2 \alpha_1^2 C_1(F_{1,t})^2 + u_{2,t} \alpha_2^2 C_2(F_{2,t})^2 - 2\rho u_{1,t} u_{2,t} \alpha_1 C_1(F_{1,t}) \alpha_2 C_2(F_{2,t}), \tag{3.8}$$

and the scaled volatility parameter u_t is approximated for $i \in \{1, 2\}$ as

$$u_t^2 = \frac{\sigma^2(t)}{C(F_t)^2} \approx \frac{p_1^2 u_{1,t}^2 + p_2^2 u_{2,t}^2 - 2\rho p_1 p_2 u_{1,t} u_{2,t}}{p^2}, \tag{3.9}$$

where

$$p_i = \alpha_i C_i(f_i), \tag{3.10}$$

$$q_i = \alpha_i C_i'(f_i), \tag{3.11}$$

$$p = p_1^2 + p_2^2 - 2\rho p_1 p_2. \tag{3.12}$$

Lastly the new Brownian differential $dB_t^{(1)}$ is given as

$$dB_t^{(1)} = \sigma(t)^{-1}\big(u_{1,t}\alpha_1 C_1(F_{1,t})dW_{1,t}^{(1)} - u_{2,t}\alpha_2 C_2(F_{2,t})dW_{2,t}^{(1)}\big) \tag{3.13}$$

The derivations of the new parameters require a few steps. First, we would like to find expressions for the expected value of the local volatility function, $b(t, x_t)^2$, in (2.5) as

$$\mathbb{E}[u_t^2|F_t = x]C(x)^2 = \mathbb{E}[\sigma^2(t)|F_t = x]. \tag{3.14}$$

To compute the conditional expectations, a first order Taylor-series approximation is applied to (3.7) and (3.9). We note that the terms in $\sigma^2(\cdot)$ and u_t^2 are linear combinations of the form $u_{i,t}u_{j,t}C_{i,t}(\cdot)C_{j,t}(\cdot)$ represented by $T^1(x_{i,j}(t))$ and $u_{i,t}u_{j,t}$ represented by $T^2(x_{i,j}(t))$, respectively. By expansion around the points $f_i, f_j, u_{i,t_0} = 1$ and $u_{j,t_0} = 1$ represented by $x_{i,j}(0)$, we have

$$\begin{aligned}
T^1(x_{i,j}(t)) &= u_{i,t}u_{j,t}C_{i,t}(F_{i,t})C_{j,t}(F_{j,t}) \\
&\approx T^1(x_{i,j}(0)) + \sum_{i,j}^{4} \frac{\partial T^1(x_{i,j}(t))}{\partial x_{i,j}(t)}(x_{i,j}(t) - x_{i,j}(0)) \\
&= C(f_i)C(f_j) \\
&\quad + (F_{i,t} - f_i)C'(f_i)C(f_j) + (F_{j,t} - f_j)C_i(f_i)C_j'(f_j) \\
&\quad + (u_{i,t} - 1)C_i(f_i)C_j(f_j) + (u_{j,t} - 1)C_i(f_i)C_j(f_j),
\end{aligned}$$

and

$$T^2(x_{i,j}(t)) = u_{i,t}u_{j,t} \approx 1 + (u_{i,t} - 1) + (u_{j,t} - 1).$$

Next, a Gaussian approximation is made to the forward F_t in (3.6) and the forwards $F_{i,t}$ in (3.1), that is we approximate their distribution as Gaussian in order to approximate the conditional expectations of the above expressions. The Gaussian dynamics are of the form

$$d\bar{F}_t = p d\bar{B}_t^{(1)}, \tag{3.15}$$

$$d\bar{F}_{i,t} = p_i dW_{i,t}^{(1)}, \tag{3.16}$$

$$d\bar{u}_{i,t} = \nu_i dW_{i,t}^{(2)}, \tag{3.17}$$

with

$$d\bar{B}_t^{(1)} = \frac{\big(p_1 dW_{1,t}^{(1)} - p_2 dW_{2,t}^{(1)}\big)}{p}, \tag{3.18}$$

possessing the correlation structure

$$\rho_1 := d\langle \bar{B}^{(1)}, W_1^{(1)} \rangle_t = \frac{p_1 - p_2\rho}{p} dt \tag{3.19}$$

$$\rho_2 := d\langle \bar{B}^{(1)}, W_2^{(1)} \rangle_t = \frac{p_1\rho - p_2}{p} dt, \tag{3.20}$$

and for $i \in \{1, 2\}$

$$\tilde{\rho}_i := d\langle \bar{B}^{(1)}, W_i^{(2)} \rangle_t = \frac{p_1\gamma_{1i} - p_2\gamma_{2i}}{p} dt. \tag{3.21}$$

Lastly, the conditional expectations of the expressions determined from the Taylor-series expansion are approximated using the new Gaussian processes as

$$\mathbb{E}[F_{i,t} - f_i | F_t = x] \approx \mathbb{E}[\bar{F}_{i,t} - f_i | \bar{F}_t = x]$$
$$\mathbb{E}[u_{i,t} - 1 | F_t = x] \approx \mathbb{E}[\bar{u}_{i,t} - 1 | \bar{F}_t = x].$$

This results in the expressions

$$\mathbb{E}[F_{i,t} - f_i | F_t = x] \approx \frac{p_i\rho_i}{p}(x - f), \tag{3.22}$$

$$\mathbb{E}[u_{i,t} - 1 | F_t = x] \approx \frac{\nu_i\tilde{\rho}_i}{p}(x - f), \tag{3.23}$$

and

$$\mathbb{E}[\sigma^2(t) | F_t = x] \approx p^2 + (x - f)A_1, \tag{3.24}$$

$$\mathbb{E}[u_t^2 | F_t = x] \approx 1 + (x - f)A_2, \tag{3.25}$$

where A_1 and A_2 are given by

$$A_1 = \frac{2(p_1^2(q_1\rho_1 + \nu_1\tilde{\rho}_1) + p_2^2(q_2\rho_2 + \nu_2\tilde{\rho}_2) - p_1p_2\rho(q_1\rho_1 + q_2\rho_2 + \nu_1\tilde{\rho}_1 + \nu_2\tilde{\rho}_2))}{p},$$
$$A_2 = \frac{2\nu_1p_1(p_1 - p_2\rho)\tilde{\rho}_1 + \nu_2p_2(p_2 - p_1\rho)\tilde{\rho}_2}{p^3}.$$

Then, the back-bone function is given as

$$C(x) \approx \sqrt{\frac{p^2 + (x - f)A_1}{1 + (x - f)A_2}}. \tag{3.26}$$

Evaluating the first derivative of this expression at f gives q as

$$q = \frac{(p_1^2q_1\rho_1 + p_2^2q_2\rho_2 - p_1p_2\rho q_1\rho_1 - p_1p_2\rho q_2\rho_2)}{p^2}.$$

Lastly, by applying the Itô formula to the variance process given by (3.9) we deduce that

$$\frac{du_t}{u_t} = \frac{p_1\nu_1\rho_1 dW_{1,t}^{(2)} - p_2\nu_2\rho_2 dW_{2,t}^{(2)}}{p},$$

which leads to

$$du_t = \nu u_t dB_t^{(2)}, \tag{3.27}$$

with

$$\nu = \frac{\sqrt{(p_1\nu_1\rho_1)^2 + (p_2\nu_2\rho_2)^2 - 2\xi p_1 p_2 \nu_1\nu_2\rho_1\rho_2}}{p},$$
$$\gamma = \frac{(p_1^2\nu_1\rho_1\gamma_{11} + p_2^2\nu_2\rho_2\gamma_{22} - p_1p_2\nu_1\rho_1\gamma_{12} - p_1p_2\nu_2\rho_2\gamma_{21}}{\nu p^2},$$

and

$$dB_t^{(2)} = (\nu p)^{-1}\big(p_1\nu_1\rho_1 dW_{1,t}^{(2)} - p_2\nu_2\rho_2 dW_{2,t}^{(2)}\big).$$

3.2 *Options on CMS Spreads*

Constant maturity swaps (CMS) are interest rate swaps where the fixed leg pays a constant time to maturity swap rate at every payment date. These liquidly traded instruments allow one to take views on future long-term rates in the yield-curve due to the fixed leg payment structure. Naturally, options on CMS spreads, the difference between the fixed and floating leg rates, are liquid too and allow for the same speculative positions to be taken.

3.2.1 *Valuation of Options on CMS Spreads*

The payoff of an option on a CMS spread on two forward rates $F_{1,t}, F_{2,t}$ with strike rate K, at maturity T, is

$$\max\{F_{1,T} - F_{2,T} - K, 0\}.$$

One commonly applied numerical method for pricing is the Gaussian copula approach introduced by Benhamou and Croissant (2007). Here, it can be shown that the payoff of this option on two correlated forward rates can be decomposed into a portfolio of digital options as

$$\max\{F_{1,T} - F_{2,T} - K, 0\} = \int_0^\infty \mathbb{I}_{[F_{1,T} > x+K]}\mathbb{I}_{[F_{2,T}<x]}dx.$$

The discounted expectation under the risk-neutral joint forward measure, P^T is computed as

$$\begin{aligned} &B(0,T)\mathbb{E}\left[\int_0^\infty \mathbb{I}_{[F_{1,T}>x+K]}\mathbb{I}_{[F_{2,T}<x]}dx\right] \\ &= B(0,T)\int_0^\infty P^T(F_{1,T} > x+K, F_{2,T} < x)dx, \end{aligned}$$

where this joint probability is computed using a Gaussian copula with the original SABR parameters. This method is static and sheds no light on the spread process dynamics, it is also time consuming because of the numerical integration and lastly, cannot be extended to CMS options with more than two forward rates.

In order to value options on CMS spreads, we make use of classic Markovian Projection where each swap rate is modelled as a SABR process with the *same* skew parameter β. The new projected SABR process is assumed to have a backbone function of the displaced diffusion form with skew parameter equal to one. This is natural since the difference between these swap rates can indeed be negative and is often seen to be. We value these claims using Hagan's perturbation expansion for the implied volatility as well as the arbitrage-free PDE approach found in Section 2.5. The prices are quoted as per market practice by their Black-implied volatilities.

3.2.2 *Black-implied volatilities and model parameters*

β	0.2	0.5	0.8	1
p_1	0.1051802	0.0325269	0.0100589	0.0046002
p_2	0.0604208	0.0245967	0.0100131	0.0055002
p	0.0841870	0.0265129	0.0089765	0.0045882
q_1	1.0518016	0.8131728	0.4023572	0.2300067
q_2	0.2416833	0.2459675	0.1602096	0.1100022
q	0.8807083	0.4397201	0.05673575	-0.02851456
ρ_1	0.8187445	0.6701975	0.4512932	0.2833546
ρ_2	0.0319202	-0.1916277	-0.4431247	-0.5971994
ν	0.7001912	0.7114202	0.7839679	0.8668244
γ	-0.2186961	-0.0653759	0.1390950	0.24841184

Tab. 3.1: Projected SABR model parameters.

Immediately in Figure 3.1 we notice a very close match for both pricing regimes for all values of the constant skew parameter used for both individual SABR rates. The smile shapes are consistent with observed market data over this wide strike range.

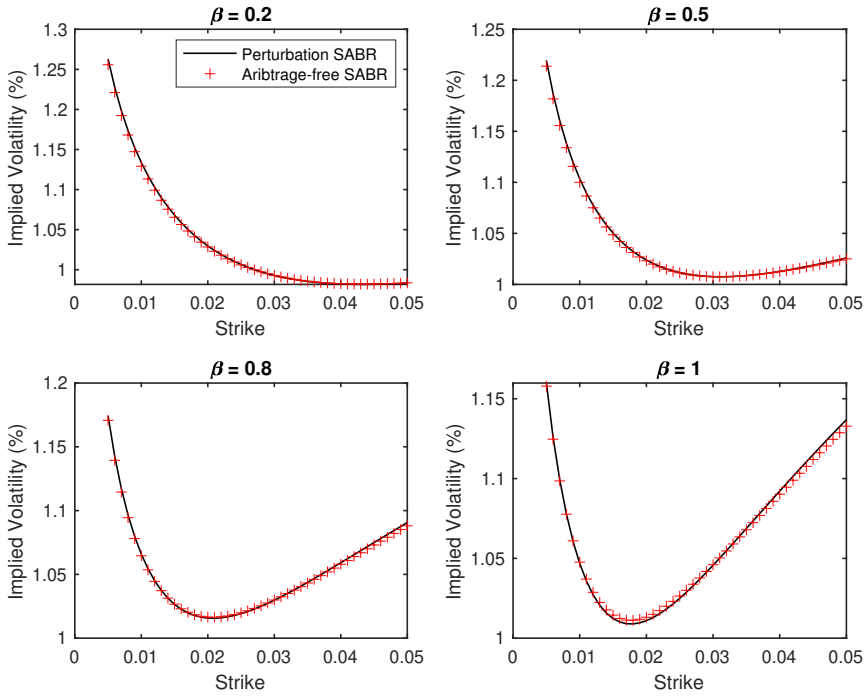

Fig. 3.1: CMS-spread option Black-implied volatility smiles for parameters: $\alpha_1 = 0.23$; $\alpha_2 = 0.11$; $f_1 = 0.02$; $f_2 = 0.05$; $\nu_1 = 0.7$; $\nu_2 = 1$; $\rho = 0.6$; $\xi = 0.7$; $\gamma_{11} = -0.4$; $\gamma_{12} = -0.2$; $\gamma_{21} = -0.2$; $\gamma_{22} = -0.4$; $T = 0.3$; $r = 0$.

SABR-Parameters
$f_{1,2} \in [0.01, 0.2]$
$\alpha_{1,2} \in [0.1, 0.25]$
$\nu_{1,2} \in [0.4, 1.2]$
$\rho \in (0, 1)$
$\gamma_{ij} \in (-1, 0)$
$T \in [0.1, 0.5]$

Tab. 3.2: Individual SABR CMS rate model parameter ranges for testing.

While it is not shown here, varying the skew parameter for either individual rate is assumed to lead to inaccurate matching. This is because the projection approximation error becomes larger when the densities of the underlying forwards are different, as will be demonstrated in the next section — this is not a problem in this example since it is reasonable to model both rates using the same skew parameter

in the case of a CMS-spread since the fixed and floating legs are usually not too far apart on the yield curve. All parameter ranges for testing in Table 3.2 are within realistic market-observable values and the new model parameters in Table 3.1 all fall within these values too.

Chapter 4

Application of Effective Markovian Projection

4.1 *Stochastic Volatility Models*

We are interested in SABR and Heston-type stochastic volatility models which take the following forms respectively

$$\begin{cases} dF_t = (F_t)^{\beta} v_t dW_t^{(1)}, & F_{t_0} = f \\ dv_t = \nu v_t dW_t^{(2)}, & v_{t_0} = \alpha \\ d\langle W^{(1)}, W^{(2)} \rangle_t = \rho dt. \end{cases} \tag{4.1}$$

$$\begin{cases} d\tilde{F}_t = \sqrt{\tilde{v}_t} \tilde{F}_t d\tilde{W}_t^{(1)}, & \tilde{F}_{t_0} = \tilde{f} \\ d\tilde{v}_t = \kappa(\Lambda - \tilde{v}_t)dt + \tilde{\nu}(t)\sqrt{\tilde{v}_t} dW_t^{(2)}, & \tilde{v}_{t_0} = \tilde{\alpha} \\ d\langle \tilde{W}^{(1)}, \tilde{W}^{(2)} \rangle_t = \tilde{\rho} dt. \end{cases} \tag{4.2}$$

Assumption 4.1. It is assumed throughout this work that the base model (4.1) parameters are constant and not asset dependant. This is a relatively benign assumption to make since constant model parameters are in some sense an average of the values over the length of the claim. If the claims under consideration are of short dated maturity then this average is a good approximation to the true, possibly time and asset-dependant value — we consider claims with a maximum maturity of 3 months.

Remark 2. One can loosen the restriction of constant model parameters as discussed in Assumption 4.1 by introducing, for example, a piece-wise constant term structure to these parameters. This is discussed by Mikhailov and Nögel (2004) where calibration of the Heston model to market data is performed in this environment.

Remark 3. Even though the SABR and Heston-type models do not possess explicit solutions, much work has been done to evaluate the probability densities of the underlying assets in each model. Exact distributions for assets following a CEV process, such as the forward in the SABR model, have been established by Lindsay and Brecher (2012) and Horvath and Reichmann (2018). Work on distributions and characteristic functions under the Heston model have been developed by Albrecher *et al.* (2007) and Dragulescu and Yakovenko (2002). These well-understood distributional properties allow for claims pricing to be studied accurately under these models.

4.2 *Projected Variance*

In order to imply equivalent Heston model parameters from the SABR models we calculate the projected variance for a specified fitting maturity and over an appropriate strike range of each model, and match them as closely as possible using each matching technique discussed.

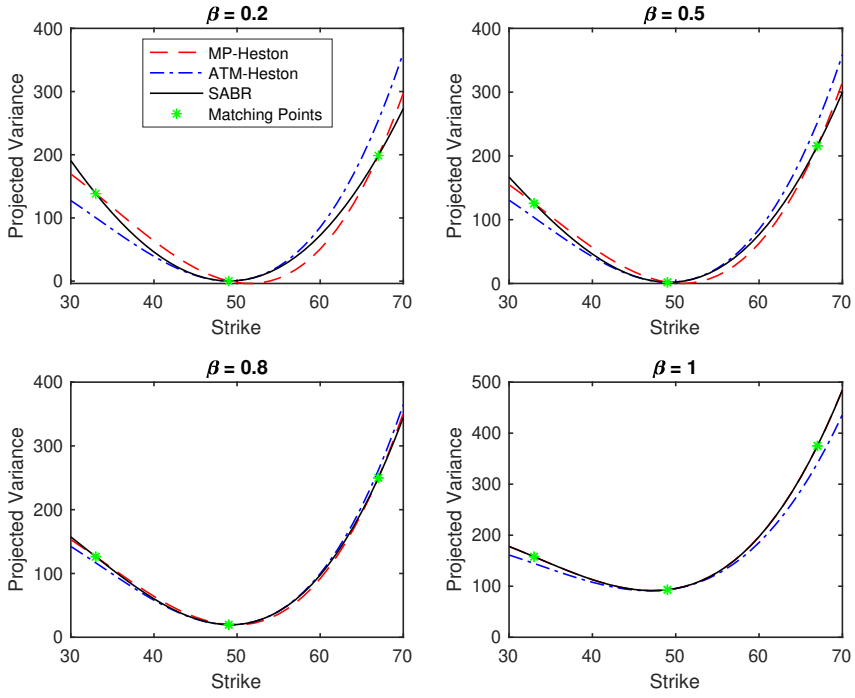

Fig. 4.1: Projected variances, σ^2_{proj}, for fitting maturity $T = 0.056$.

4.3 *Projection Model Parameters*

In order to solve for $\tilde{\alpha}$ in (4.2) we use the definition in (2.8) and find the zero(s) of the equation

$$\tilde{\alpha}e^{-\left(\tilde{c}(t)-\tilde{b}(t)\right)\tilde{\tau}(t)} - \hat{a}(t) = 0.$$

Once $\tilde{\alpha}$ is computed, $\tilde{\rho}$ and $\tilde{\nu}$ in (4.2) are given as

$$\tilde{\nu} = \sqrt{\frac{-\left(\tilde{c}(t)-\frac{6\tilde{b}(t)^2}{T\left(1-e^{-\kappa T}\right)}\left(\frac{1}{\kappa}\left(1-e^{-\kappa T}\right)-T\right)-\left(2\kappa\frac{\tilde{b}(t)}{\left(1-e^{-\kappa T}\right)}\right)^2\left(-\frac{1}{\kappa}Te^{-\kappa T}+\frac{1}{\kappa^2}\left(1-e^{-\kappa T}\right)\right)\right)2\kappa\tilde{\alpha}^2T^2}{\frac{1}{2\kappa}\left(1-e^{-2\kappa T}\right)-\frac{1}{\kappa}\left(1-e^{-\kappa T}\right)}},$$

and

$$\tilde{\rho} = \frac{2\tilde{b}(t)\kappa\tilde{\alpha}T}{\tilde{\nu}(1-e^{-\kappa T})},$$

by implication in the expressions for the coefficients given in Appendix A. Lastly, κ is computed by minimising the difference between the projected variances of each model. As per Assumption A.1, we set $\Lambda = \tilde{\alpha}$ for all $t \in [0, T]$. All projection model parameters are solved, subject to satisfying 'Feller's square-root condition'

$$2\kappa\Lambda > \nu^2.$$

This condition being met guarantees a unique solution to the SDE governing the variance dynamics in (4.2) and is important to guarantee stability in pricing schemes. A proof of this result can be found in Gikhman (2011).

In Figure 4.1 we notice that for all values of β, the ATM fitting of the projected variance becomes poorer at the far ITM and OTM values of the forward. We notice that the MP-matching technique produces a better fit at these values. The fitting becomes better for both matching algorithms the closer the skew parameter approaches 1 and is an almost perfect match for MP-matching. This is likely because when $\beta = 1$, the terminal (fitting maturity) densities of the forward in each model is log-normal and the approximation error of the densities used in the expressions for the projected variances for each model in (2.6) are similar. The base and projection model densities are also narrowly concentrated around the ATM-strike value as shown in Felpel *et al.* (2021) Figure 1. Because of this, the ill-fitting of the projected variances at the wings has a large impact on the projection model parameters since the transition densities of these models is used directly in their estimation. Quantification of the error analysis involved in computing the projected variances for differing ATM, ITM and OTM values of the forward is discussed extensively in Hagan *et al.* (2018) and Felpel *et al.* (2022).

For comparison in Figure 4.2, we show the projected variances for a maturity of five years.

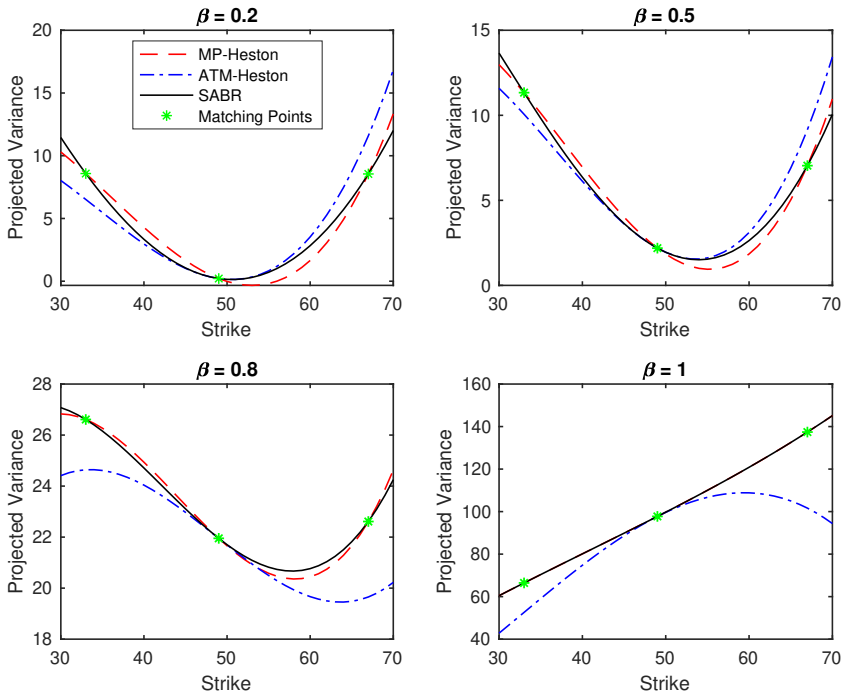

Fig. 4.2: Projected variances, σ^2_{proj}, for fitting maturity $T = 5$.

Immediately we notice that the projected variances for both matching techniques fit more poorly for $\beta < 0.8$ as compared to Figure 4.1. The ATM-matching at the far ITM and OTM strikes is also less accurate than for the shorter-dated maturity. Assumption 4.1 is clearly not accurate for these longer maturities and time-dependence of the base model parameters should be introduced if claims are to be priced for these times.

It is also worthwhile noting that the selection of the ATM forward value heavily affects the closeness of fit of the projected variance. An error analysis of the projected variances can be found in Felpel *et al.* (2022) Table 4. The choice here was done based on the visual best fit.

4.4 *Heston Parameters*

β	$\tilde{\alpha}(10^{-4})$	$\tilde{\nu}(10^{-2})$	$\tilde{\rho}$	κ
0.2	0.7911316	0.6240273	-0.1490615	3.79949951
0.5	8.1734546	2.0208805	-0.1705124	3.8058472
0.8	84.3975505	5.8459250	-0.1921789	1.6730347
1	398.6667476	2.5084307	-0.2923817	25.0922241

Tab. 4.1: ATM-Heston parameters for SABR parameters: $f = 49$; $T = 0.056$; $\alpha = 0.15$; $\nu = 0.02$; $\rho = -0.4$.

β	$\tilde{\alpha}(10^{-4})$	$\tilde{\nu}(10^{-2})$	$\tilde{\rho}$	κ
0.2	0.7918686	1.4165718	-0.8999746	5.1250000
0.4	0.8.1778252	2.3850659	-0.45446235	5.2500000
0.5	84.4635239	6.7816364	-0.2200709	4.4707031
1	400.4469871	14.3812947	-0.1275631	4.9995117

Tab. 4.2: MP-Heston parameters for SABR parameters: $f = 49$; $T = 0.056$; $\alpha = 0.15$; $\nu = 0.02$; $\rho = -0.4$

SABR-Parameter
$f \in [48, 52]$
$\alpha \in [0.05, 0.25]$
$\nu \in [0.001, 0.5]$
$\rho \in (-1, 0)$
$T \in [0.019, 0.25]$

Tab. 4.3: SABR parameter ranges for testing.

The parameter ranges used for testing in Table 4.3 all fall within realistic values and were chosen for this reason. One notices that as β approaches unity, the projection model parameter values in Tables 4.1 and 4.2 become more realistic in a market-observable sense. The Heston parameters ν and α for $\beta = 0.2$ and $\beta = 0.4$ are unrealistically small. These are the values that match the projected variances best but should not be thought of as a true representation of what would be observed from market data.

4.5 *Call Option Prices*

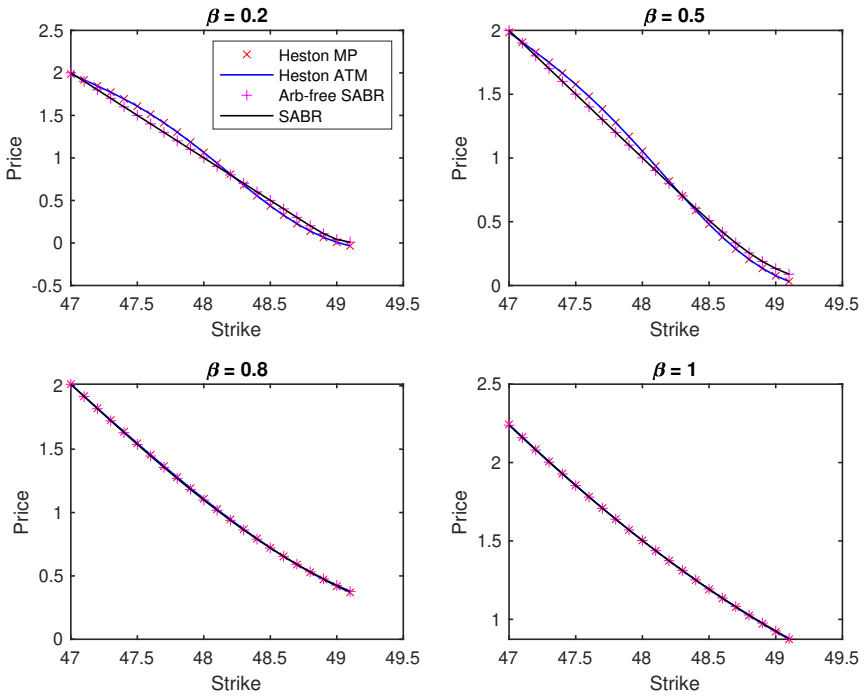

Fig. 4.3: Vanilla European call prices under Heston and SABR Models.

We notice here that the call prices in Figure 4.3 for both matching techniques when $\beta = 0.2$ and $\beta = 0.5$ are inaccurate in that for certain strikes the value falls below zero, and do not match either SABR price closely. This is due to the ill-matching of the projected variances and consequently inaccurately projected model parameters, along with the sensitivity of the characteristic function pricing technique to these model parameters. There is also oscillatory behaviour in the Heston prices due to this same sensitivity and is likely also due to the effect of strike values and maturity of the claim. As β approaches unity this behaviour vanishes and the option prices match closely as expected.

4.6 *CMP Comparison*

Comparing these prices and projected variances for $\beta < 1$ to the prices implied by Figure 3.1, we can immediately see that there is no ill-matching of the prices when $\beta < 1$. This is because each underlying SABR model used to price these options on CMS spreads shares the *same* skew parameter and the same underlying probability

density — the approximation error in the density of the asset in the projected model is consistent. In the case of EMP, only when β approaches unity do the densities of the underlying Heston and SABR assets match more closely which gives rise to a better match of the option prices.

4.7 *Monte-Carlo Heston Prices and Pricing Error Comparison*

As a comparison, we show MP Heston prices computed using a discretised Milstein Scheme (Appendix A) and Monte-Carlo simulation with the same option parameters. We then compare the pricing errors of the Heston prices from both matching algorithms together with the Monte-Carlo prices, with the perturbation expansion SABR prices.

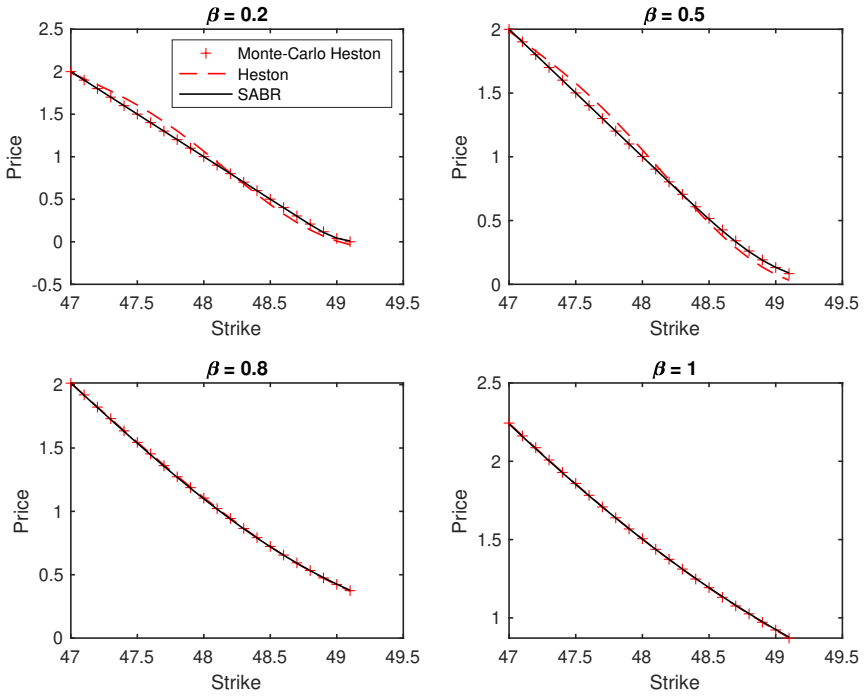

Fig. 4.4: MP-matching Monte-Carlo Heston call prices.

In Figure 4.4 we notice that the Monte Carlo prices for all values of β match almost perfectly with the SABR prices. This shows the sensitivity of the characteristic function pricing technique to model parameters.

The main advantages of EMP in this context is that it enables one to utilize the calibration efficiency of the SABR model and the characteristic function pricing efficiency of the Heston model with a single set of model parameters. We see here that this pricing technique is only an advantage if the model parameters are implied extremely accurately and realistically from the base model. In other words, if the projected variances of both models do not match well (i.e., when $\beta < 0.8$), this pricing technique is no longer an advantage and inaccurate/unstable pricing is witnessed.

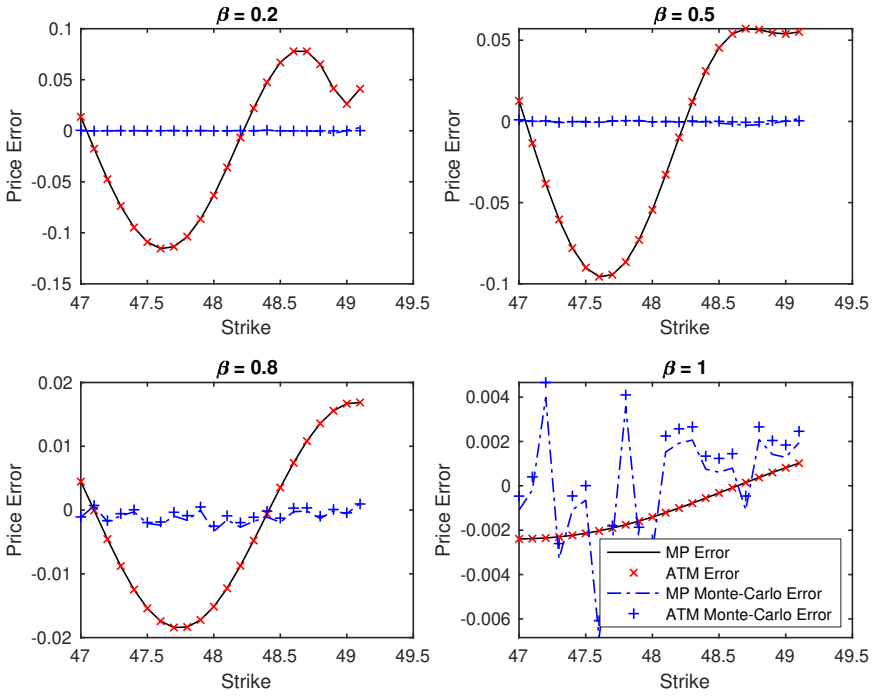

Fig. 4.5: Pricing error comparison for various pricing schemes and matching algorithms.

In Figure 4.5, for $\beta < 0.8$, we see the MP and ATM Heston price errors are consistent with one-another while the Monte-Carlo price errors for both matching algorithms is far smaller. When $\beta \geq 0.8$, the oscillatory behaviour of the Monte-Carlo pricing error is observed while the Heston characteristic function pricing becomes very accurate and performs better than the Monte-Carlo scheme — clearly the efficacy of the EMP technique in this context becomes clear.

Chapter 5

Conclusion

In this dissertation the theory behind classic Markovian Projection and Effective Markovian Projection was discussed. Classic Markovian Projection was used to value options on CMS spreads under the SABR model and Effective Markovian Projection was used in a novel way to obtain equivalent Heston model parameters from a range of SABR models with varying skew parameters. The SABR and implied Heston parameters were used to price European call options with specified contract parameters using a variety of pricing techniques. Using these prices, implied parameters, option prices obtained using CMP and the efficacy and realism of the EMP technique to Heston and SABR models was discussed. Specifically, the implied Heston parameters become more realistic as β approaches unity or as the underlying forward densities in the SABR and Heston models agree. This is observed in the plots of projected variances as well as parameter tables and backed up by the close price matching of options on CMS spread using CMP wherein the densities of both underlying rates is always the same. The Heston characteristic function pricing scheme is unstable, giving certain negative option values, for β less than 0.8. This is seen by comparing to Monte-Carlo prices of these claims under equivalent contract parameters. It can be concluded that this technique increases in accuracy and efficacy when the probability densities of the underlying forward values are the same and can lead to poor results when these densities do not match closely.

A possible solution to this problem is the introduction of a correction algorithm which corrects for the difference in probability density between the two models. This would potentially allow for a closer approximation of the projected variances and thus give more accurate option prices and allow for pricing over a wider strike range.

Bibliography

Albrecher, H., Mayer, P., Schoutens, W. and Tistaert, J. (2007). The little Heston trap, *Wilmott* **2007**(1): 83–92.

Benhamou, E. and Croissant, O. (2007). Local time for the SABR model: Connection with the 'complex' Black- Scholes and application to CMS and spread options, *Available at SSRN 1064461* .

Breeden, D. T. and Litzenberger, R. H. (1978). Prices of state-contingent claims implicit in option prices, *Journal of business* **51**(4): 621–651.

Derman, E. and Kani, I. (1994). Riding on a smile, *Risk* **7**(2): 32–39.

Dragulescu, A. A. and Yakovenko, V. M. (2002). Probability distribution of returns in the Heston model with stochastic volatility, *Quantitative finance* **2**(6): 443.

Dupire, B. (1994). Pricing with a smile, *Risk* **7**(1): 18–20.

Felpel, M., Kienitz, J. and McWalter, T. A. (2021). Effective stochastic volatility: Applications to ZABR-type models, *Quantitative Finance* **21**(5): 837–852.

Felpel, M., Kienitz, J. and McWalter, T. A. (2022). Effective markovian projection: application to CMS spread options and mid-curve swaptions, *Quantitative Finance* **22**(6): 1169–1192.

Gikhman, I. I. (2011). A short remark on Feller's square root condition, *Available at SSRN 1756450* .

Gil-Pelaez, J. (1951). Note on the inversion theorem, *Biometrika* **38**(3-4): 481–482.

Gyöngy, I. (1986). Mimicking the one-dimensional marginal distributions of processes having an Itô differential, *Probability theory and related fields* **71**(4): 501–516.

Hagan, P. S. (2015). Conservative schemes for solving 1d PDES, *Available at Researchgate* .

Hagan, P. S., Kumar, D., Lesniewski, A. S. and Woodward, D. (2014). Arbitrage-free SABR, *Wilmott* **2014**(69): 60–75.

Hagan, P. S., Kumar, D., Lesniewski, A. S. and Woodward, D. E. (2002). Managing Smile Risk, *The Best of Wilmott* **1**: 249–296.

Hagan, P. S., Lesniewski, A. S. and Woodward, D. E. (2018). Implied volatility formulas for Heston models, *Wilmott* **2018**(98): 44–57.

Heston, S. L. (1993). A closed-form solution for options with stochastic volatility with applications to bond and currency options, *The review of financial studies* **6**(2): 327–343.

Horvath, B. and Reichmann, O. (2018). Dirichlet forms and finite element methods for the SABR model, *SIAM Journal on Financial Mathematics* **9**(2): 716–754.

Kienitz, J. and Wittke, M. (2010). Option valuation in multivariate SMM/SABR models (with an application to the CMS spread), *Available at SSRN 1469554* .

Kumar, K. S. (2013). A class of degenerate stochastic differential equations with non-Lipschitz coefficients, *Proceedings-Mathematical Sciences* **123**(3): 443–454.

Lawson, J. and Swayne, D. (1976). A simple efficient algorithm for the solution of heat conduction problems, *Proceedings of the 6th Manitoba Conference on Numerical Mathematics*, p. 250.

Le Floc'h, F. and Kennedy, G. J. (2014). Finite difference techniques for arbitrage free SABR, *Available at SSRN 2402001* .

Lindsay, A. E. and Brecher, D. (2012). Simulation of the CEV process and the local martingale property, *Mathematics and Computers in Simulation* **82**(5): 868–878.

McWalter, T. A. (2021). Numerical Methods in Finance II, Lecture Notes.

Mikhailov, S. and Nögel, U. (2004). *Heston's stochastic volatility model: Implementation, calibration and some extensions*, John Wiley and Sons.

Oskendal, B. (2000). *Stochastic differential equations (5ed)*, Springer.

Piterbarg, V. (2006). Markovian projection method for volatility calibration, *Available at SSRN* **906473**.

Piterbarg, V. V. (2005). Stochastic volatility model with time-dependent skew, *Applied Mathematical Finance* **12**(2): 147–185.

Appendix A

Effective Markovian Projection

A.1 *Projected Variance Coefficient Functions for Heston and SABR models*

Various assumptions are made in the derivations of the coefficient functions in (2.6) by Felpel *et al.* (2021) for SABR and Heston models.

Assumption A.1. The drift component $\mu(\cdot)$ in (1.1) is differentiable and a solution $Y(t, t_0, \alpha)$ to the PDE

$$\begin{aligned} \partial_t Y(t, t_0, \alpha) &= \mu(Y(t, t_0, \alpha)), \\ Y(t, t, \alpha) &= \alpha, \\ Y(t_0, t_0, \alpha) &= \alpha, \end{aligned}$$

exists.

Assumption A.2. The solution $Y(t, t_0, \alpha)$ is differentiable and has inverse function such that

$$Y(t, t_0, \alpha) = a \iff \alpha = y(t_0, t, a).$$

Assumption A.3. The functions

$$\begin{aligned} X(t, t_0, \alpha) &= \partial_\alpha Y(t, t_0, \alpha), \\ Z(t, u) &= y(u, t, Y(t, t_0, \alpha)), \\ z(F) &= \int_f^F \frac{1}{C(u)} du, \\ s(t) &= \int_{t_0}^t y(u, t, Y(t, t_0, \alpha))^2 du, \end{aligned}$$

and

$$\psi(t, u, Z) = \nu(Z(t, u)) Z(t, u) X(t, u, Z(t, u)),$$

are well-defined and the inverse $X(t, u, Z(t, u))^{-1}$ exists.

With these assumptions the following general integral functions are defined:

$$
\begin{aligned}
I_1(t) &= \rho \int_{t_0}^{t} \psi(t,u,Z)du, \\
I_2(t) &= 2\int_{t_0}^{t} \nu(z(t,u))^2 X(t,u,Z(t,u))^2 \int_{u}^{t} Z(t,\nu)X(t,\nu,Z(t,\nu))^{-1}d\nu du, \\
I_3(t) &= \rho \int_{t_0}^{t} \psi(t,u,Z) \int_{u}^{t} Z(t,\nu)X(t,\nu,Z(t,v))^{-1}d\nu du, \\
I_4(t) &= \rho^2 \int_{t_0}^{t} \psi(t,u,Z) \int_{u}^{t} \partial Z(\psi(t,\nu,Z))X(t,\nu,Z(t,\nu))^{-1}d\nu du, \\
I_5(t) &= \int_{t_0}^{t} \nu(Z(t,u))^2 X(t,u,Z(t,u))^2 du.
\end{aligned}
$$

With these integral functions the coefficient functions are defined as

$$
\begin{aligned}
a(t) &= Y(t,t_0,\alpha), \\
b(t) &= \frac{1}{a(t)s(t)} I_1(t), \\
c(t) &= b(t)^2 + \frac{1}{a(t)s(t)^2} I_2(t) - \frac{6b(t)}{s(t)^2} I_3(t) + \frac{2}{a(t)s(t)^2} I_4(t), \\
G(t) &= -s(t)c(t) - s(t)b(t)\Gamma_0 + \frac{1}{a^2} I_5(t),
\end{aligned}
$$

where

$$\Gamma_0 = -C'(f).$$

We use a special case of the Heston Model here where $\Lambda = v_{t_0} = \alpha$ for all $t \in [0,T]$. For the Heston model the following integral functions are defined for ease of notation as

$$
\begin{aligned}
\tau(t) &= \int_0^t \hat{V}(u)du = \alpha t, \\
D(u,t) &= \int_u^t e^{-\int_u^v \kappa dw} dv = \frac{-1}{\kappa}\left[e^{-\kappa(t-u)} - 1\right],
\end{aligned}
$$

where $\hat{V}$ is the expected value of the variance which is given by α. Then,

$$
\begin{aligned}
I_1(t) &= \int_0^t \rho\nu\alpha e^{-\int_u^t \kappa dv} du = \frac{\rho\nu\alpha}{\kappa}\left[1 - e^{-\kappa t}\right], \\
I_2(t) &= \int_0^t \rho\nu\alpha D(u,t)du = \frac{-\rho\nu^2\alpha}{\kappa}\left[\frac{1}{\kappa}(1 - e^{-\kappa t}) - t\right], \\
I_3(t) &= \int_0^t \nu^2\alpha D(u,t) e^{-\int_u^t \kappa dv} du = \frac{-\nu^2\alpha}{\kappa}\left[\frac{1}{2\kappa}\left(1 - e^{-2\kappa t}\right) - \frac{1}{\kappa}\left(1 - e^{-\kappa t}\right)\right],
\end{aligned}
$$

and

$$
I_4(t) = \int_0^t \rho\nu\alpha e^{-\int_u^t \kappa dv} \int_u^t \rho\nu dw du = \alpha\rho^2\nu^2\left[\frac{-1}{\kappa} t e^{-\kappa t} + \frac{1}{\kappa^2}\left(1 - e^{-\kappa t}\right)\right].
$$

The Heston coefficient functions are then given by

$$b(t) = \frac{I_1(t)}{2\alpha\tau(t)}, \qquad c(t) = \frac{I_3(t)}{2\alpha\tau^2(t)} - 3b(t)\frac{I_2(t)}{\tau^2(t)} + \frac{I_4(t)}{\alpha\tau^2(t)},$$

and

$$G(t) = [-b(t)\Gamma_0 + c(t)]\tau(t) = -[c(t) - b(t)]\tau(t).$$

The following integral functions are given explicitly for the general SABR model as

$$I_1(t) = \rho\nu\alpha t, \qquad I_2(t) = \nu^2\alpha t,$$
$$I_3(t) = \frac{\rho\nu\alpha^2 t}{2}, \qquad I_4(t) = \frac{\rho^2\nu^2\alpha t^2}{2},$$

and

$$I_5(t) = \nu\alpha^2 t.$$

A.2 *Discretised Milstein Scheme for Heston Monte-Carlo Pricing*

The discretised Milstein scheme for the evolution of the forward, F, indexed by i is as follows

$$\hat{F}_i = \begin{cases} f & i = 0 \\ \hat{F}_{i-1}\exp\left(\left(r - \frac{1}{2}\hat{v}_{i-1}\right)\Delta t + \sqrt{\hat{v}_{i-1}}\sqrt{\Delta t}Z_{F,i}\right) & i > 0 \end{cases}$$

Where,

$$\hat{v}_i = \begin{cases} \alpha & i = 0 \\ \left(\hat{v}_{i-1} + \kappa(\Lambda - \hat{v}_{i-1})\Delta t \right. \\ \left. +\nu\sqrt{\hat{v}_{i-1}}\sqrt{\Delta t}Z_{v,i} + \frac{1}{4}\nu^2(Z_{v,i}^2 - 1)\Delta t\right)^+ & i > 0 \end{cases}$$

The standard normal random variables, $Z_{\cdot,i}$ are generated with correlation ρ. Then the price of a claim, V at maturity T is

$$V(K) = \mathbb{E}[(\hat{F}_T - K)^+]$$